Automation of chamfering by an industrial robot; for the case of machined hole on a cylindrical workpiece

Proceedings of the 1998 IEEE
International Conference on Robotics & Automation
Leuven, Belgium • May 1998

Automation of Chamfering by an Industrial Robot; For the Case of Machined Hole on a Cylindrical Workpiece

Naoki Asakawa, Kenji Toda and Yoshimi Takeuchi

Department of Mechanical and Control Engineering
University of Electro-Communications, Chofu, Tokyo, 182-8585 Japan

Abstract

The study deals with the automatic chamfering for the case of a machined hole on a cylinder on the basis of CAD data, using an industrial robot. As a chamfering tool, a rotary-bar driven by an electric motor is mounted to the arm of the robot having six degreesoffreedom in order to give an arbitrary position and attitude to the tool. The robot control command converted from the chamfering path is transmitted directly to the robot. From the experimental results, the system is found effective to remove a burr along the edge of a hole on a cylindrical metallic workpiece.

1 Introduction

The chamfering performed to deburr the edge of a workpiece after the drilling process is necessary to obtain workpieces with a smooth and clean edge. The requirement of automation of chamfering has strongly increased as the work is done in a contaminated environment. Therefore, industrial robots have been employed to automate the chamfering and / or deburring. However, the characteristics of burrs, whose shape are not necessarily constant, make it difficult to automate the operation.

A study copes with a variety of burr shapes by use of a laser-sensor to measure the shape in advance [1], and the others resolve the problem in terms of a feedback control and a compliance control to stabilize deburring condition [2, 3, 4, 5, 6]. These methods focused not on the path generation of itself but on the improvement of the tool path. While most of robots are controlled under a teaching-playback mode, some studies used CAD/CAM system to realize high-leveled automation [7, 8]. However, they did not consider the attitude of the robot arm, but considered the attitude of the tool. When an operation is performed with a multi-axis robot, it is important to keep the movement of the robot within the axis limit.

In the study, we treat a drilled hole on a cylindrical workpiece, frequently seen as cross-holes in a main spool of oil pressure parts, a hole on a cam shaft of a car and so on. Since the edge of the hole is not a simple circle but a 3-dimensional curved line, the chamfering has been conducted by skilled workers with a file, a whetstone or a rotary-bar.

To automate the chamfering, we introduce a robot with six-degrees-of-freedom on the basis of CAD/CAM system. As a result, the system is found effective to remove a burr along the edge of a hole on a cylindrical workpiece.

2 System Configuration

The system configuration is illustrated in Fig. 1. The robot having six degrees of freedom (Fanuc : Robot S-700), shown in Fig. 2, is used. The positioning accuracy of the robot is 0.2 mm, the load capacity is 300 N, and the arm is 2600 mm in length. As a chamfering tool, a motor with rotary-bar shown in Fig. 3 is attached to the robot arm. A touch sensor is mounted at the robot arm by a detachable holder as well as the chamfering tool to recognize the position and attitude of the workpiece. The workpiece shape is defined by use of 3D-CAD system (Ricoh : Design base). The chamfering path is generated by use of the our own CAM system on EWS (Sun : Sparc station), based on the CAD data. The robot control data generated on a personal computer (NEC : PC-98) with reference to the chamfering path are transferred to the robot controller through a RS-232-C. Then, the chamfering tool mounted to the robot arm starts chamfering.

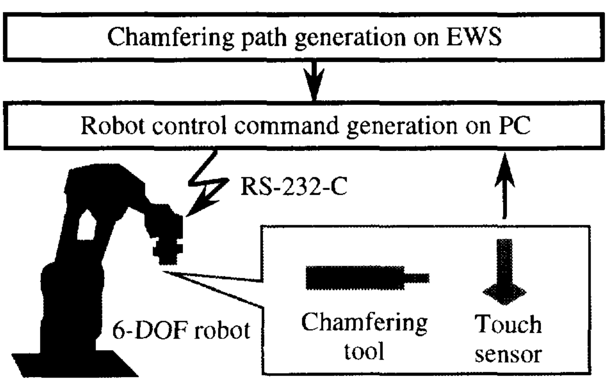

Fig. 1 Configuration of the system

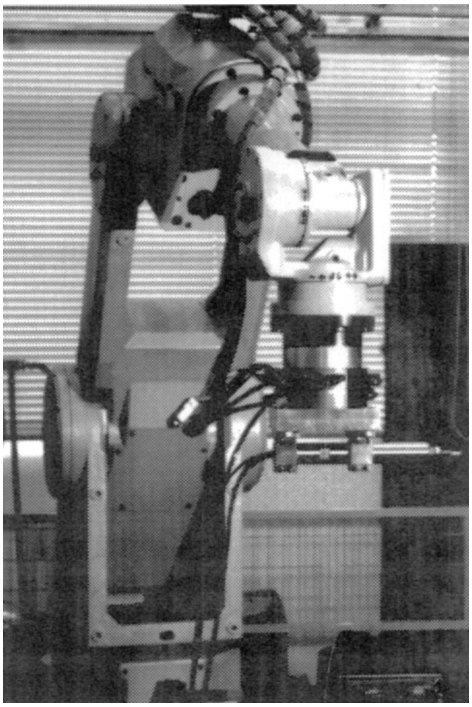

Fig. 2 Whole view of the robot used in the system

3 Basic Chamfering Model

3.1 Workpiece

Let us assume an edge with a right angle consisting of planes *A* and *B*, which is chamfered with 45 degree, as shown in Fig. 4. The symbols are as follows;

- P — Chamfering point
- ***N*** — Normal vector at each chamfering point
- ***F*** — Feed vector to the next chamfering point
- ***D*** — Tool axis vector

X_n means the *n*-th *X* in the figure. The parameters are called "workpiece surface data".

3.2 Chamfering Tool

The chamfering tool used in the system is modeled and

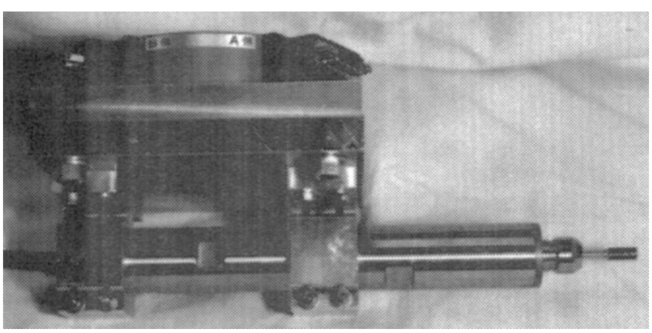

Fig. 3 Chamfering tool used in the system

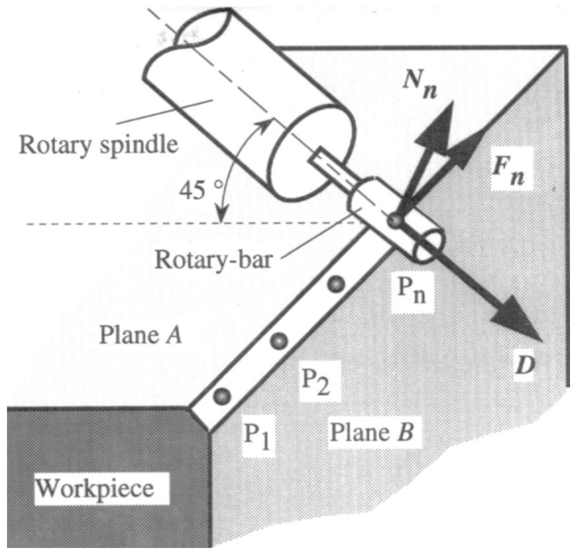

Fig. 4 Workpiece surface data on a basic chamfering model

attached to the robot as shown in Fig. 5,
where

- ***D*** — Tool axis vector
- T_f — Functional tool vector
- T_g — Geometrical tool vector

These parameters are called "tool attitude data". The tool vector ***D*** is parallel to the rotational axis of the chamfering tool, and is perpendicular to the vector N_{arm}, which is also parallel to the center axis of the robot arm.

Since the tool can machine a workpiece with any side part of the rotary-bar pushed against the workpiece, the functional tool vector T_f, representing the tool pushing direction, can be defined as an arbitrary vector within a plane *M*, whose normal is vector ***D***. Considering the function of tool, the tool requires five degrees of freedoms.

On the other hand, the robot used in the system has six axes, which give the tool an arbitrary attitude. The robot attitude can be defined by appointing two vectors, the tool axis vector ***D*** and the geometrical tool vector T_g parallel to N_{arm}, considering the tool holder.

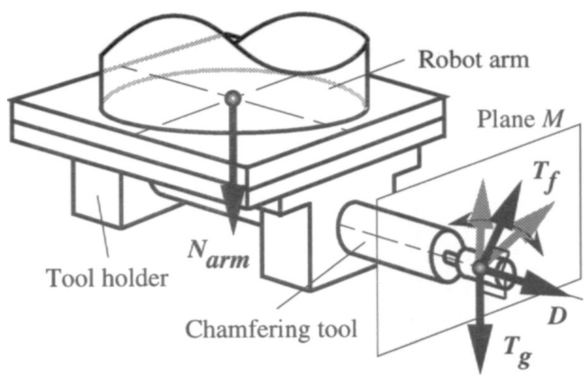

Fig. 5 Vectors for tool attitude

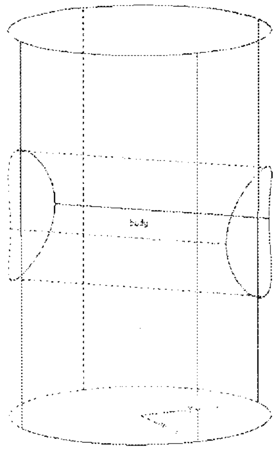

Fig. 6 CAD model of a workpiece

The tool path generation is to converte a series of workpiece surface data to a series of tool attitude ones.

4 Main-processor

4.1 Generation of Cylindrical Workpiece Surface Data

An example of the defined objective shape of cylindrical workpiece is shown in Fig. 6. The shape is a simplified model of a hole through a cylinder and is obtained by the subtractive operation between two cylinders on CAD system. Let us apply the above model to obtain the workpiece surface data for chamfering.

In Fig. 7, the cylinder *A*, the base cylinder, penetrates the cylinder *B* by drilling. The circle *b* is obtained as a cross section between the cylinder *B* and the plane *L* perpendicular

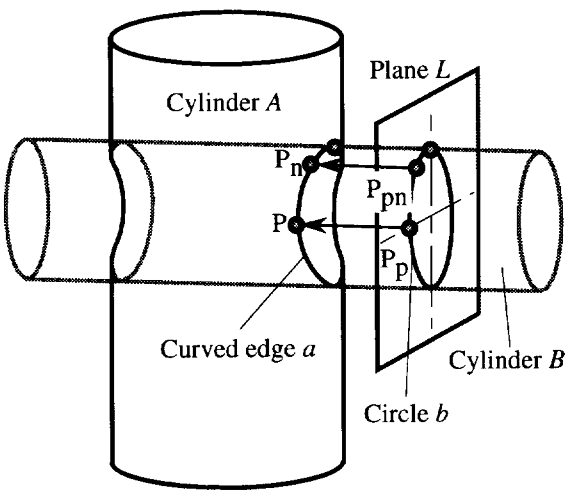

Fig. 7 A cylindrical workpiece model

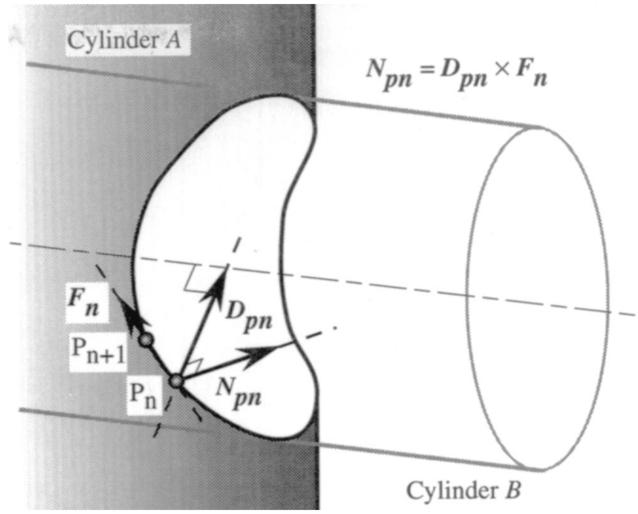

Fig. 8 Generation of chamfering points

to the cylinder *B*. The curved edge *a* is an edge of the cross section between the cylinder *A* and *B*. The circle *b* is equally divided by points P_p, depending on a chamfering condition. The chamfering point P is the projected one of P_p onto the curved edge *a*.

As shown in Fig. 8, $\boldsymbol{D_{pn}}$ and $\boldsymbol{F_n}$ are the vectors directing from P_n to the center axis of the cylinder *B* and from P_n to P_{n+1} respectively. An outer product of $\boldsymbol{D_{pn}}$ and $\boldsymbol{F_n}$, corresponds to the normal vector of the plane *A* in Fig. 4. As shown in Fig. 9, the vectors $\boldsymbol{D_n}$ and $\boldsymbol{N_n}$ are obtained by revolving $\boldsymbol{D_{pn}}$ and $\boldsymbol{N_{pn}}$ around $\boldsymbol{F_n}$ by 45 degrees respectively. As a result, the vectors obtained correspond to the normal vector $\boldsymbol{N}$, the feed vector $\boldsymbol{F}$ and the tool axis vector $\boldsymbol{D}$ in Fig. 4 at the chamfering point P. An example of the workpiece surface data displayed on CRT is shown in

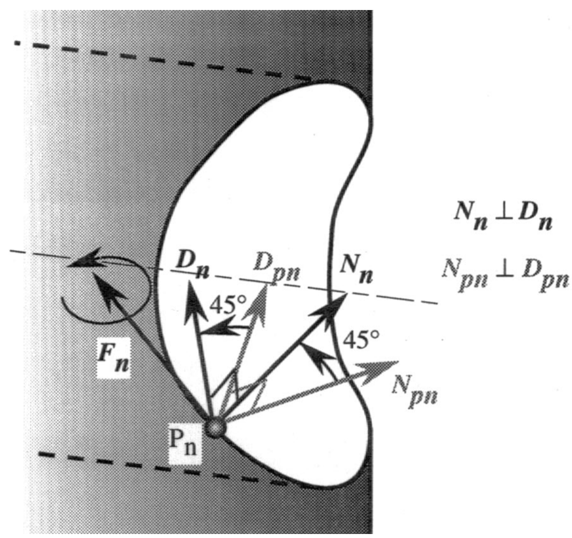

Fig. 9 Generation of tool vectors

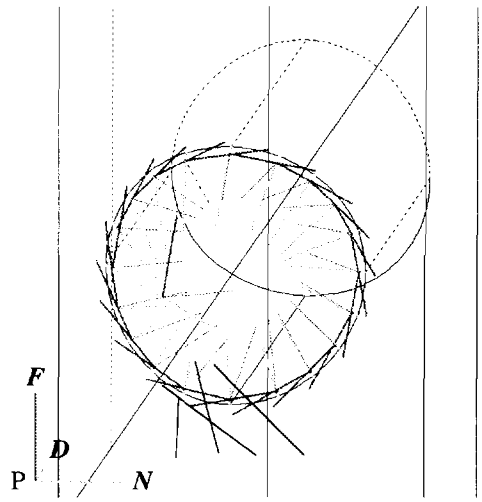

Fig. 10 Workpiece surface information

Fig. 10.

4.2 Conversion to the Tool Path

In this step, the workpiece surface data such as the chamfering point P, the normal vector $\boldsymbol{N}$, the feed vector $\boldsymbol{F}$ and the tool axis vector $\boldsymbol{D}$ are converted to the tool attitude data such as the tool axis vector $\boldsymbol{D}$, the geometrical tool vector $\boldsymbol{T_g}$ and the functional tool vector $\boldsymbol{T_f}$. The vector $\boldsymbol{D}$ in the workpiece surface data is the same one in the tool attitude data. The vector $\boldsymbol{T_f}$ standing for the tool pushing direction is obtained as an inverse vector of $\boldsymbol{N}$. The problem is how to relate $\boldsymbol{T_f}$ to $\boldsymbol{T_g}$.

As a simple method, let us use $\boldsymbol{T_f}$ as $\boldsymbol{T_g}$. The tool path generated by the method is shown in Fig. 11. With the method, however, the change in $\boldsymbol{N}$ directly influences $\boldsymbol{T_g}$. When the robot is driven by $\boldsymbol{T_g}$, as shown in Fig. 12, the change in the robot attitude becomes large, and makes the robot joints easily reach to the rotational angle limit. It is due to the direct generation of $\boldsymbol{T_g}$ ($=\boldsymbol{T_f}$) from an inverse

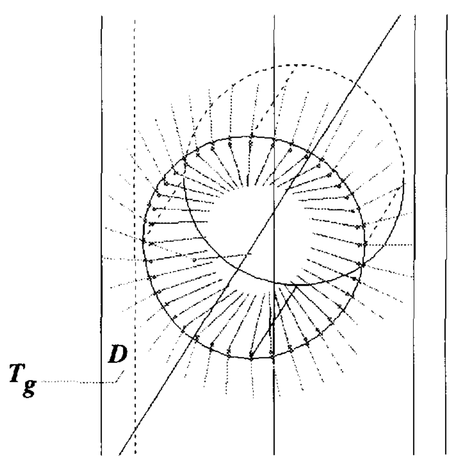

Fig. 11 Tool path based on the simple method

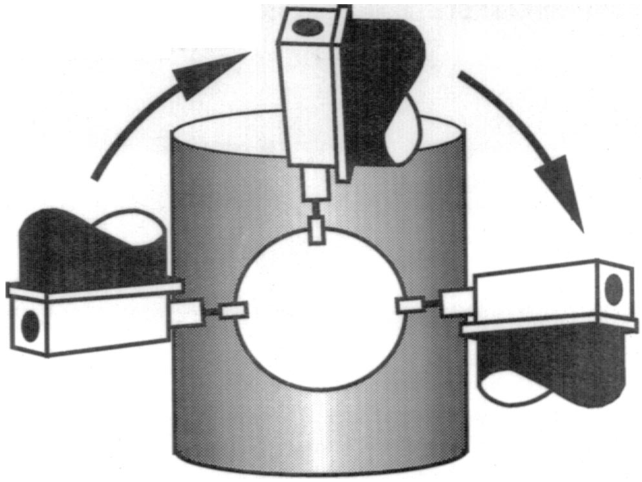

Fig. 12 Change in the robot attitude based on the simple method

vector of $\boldsymbol{N}$.

As is mentioned above, $\boldsymbol{T_f}$ can be defined as an arbitrary vector within a plane having the vector $\boldsymbol{T_f}$ as its normal vector. When $\boldsymbol{T_f}$ is fixed, the tool can rotate around $\boldsymbol{D}$. Therefore, $\boldsymbol{T_g}$ can arbitrarily be selected from $\boldsymbol{T_f}$, which exists infinitely around $\boldsymbol{D}$. This is because five degrees of freedom is enough for the tool though a robot has six degrees of freedom. In other words, a degree of freedom is redundant.

Based on the above characteristics, $\boldsymbol{T_f}$ can be converted to $\boldsymbol{T_g}$, considering an attitude of the robot. The concept is realized by making selection of $\boldsymbol{T_g}$ so that $\boldsymbol{T_f}$ may make the changes in the robot attitude as small as possible.

Figure 13 illustrates the view of vector $\boldsymbol{T_f}$ from the center axis direction of the cylinder B. The angle between

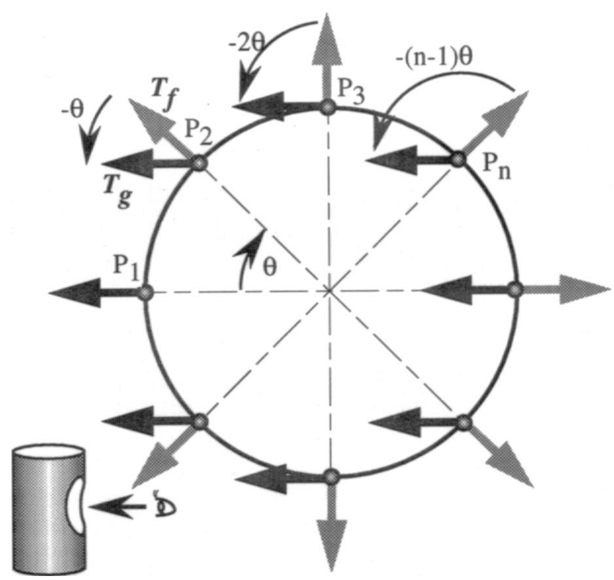

Fig. 13 Concept of a new method to generate the vector T_g from the vector T_f

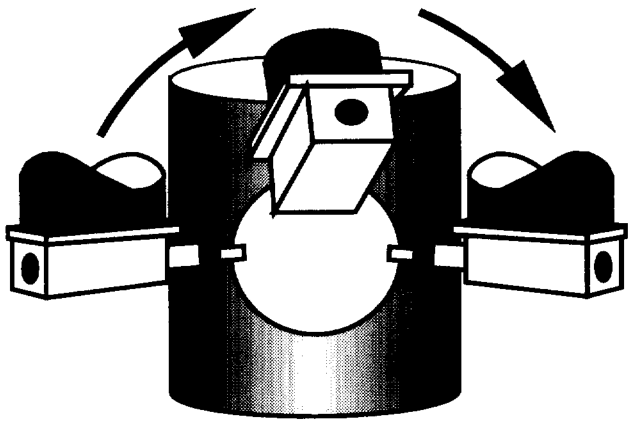

Fig. 14 Change in the robot attitude based on the new method

the horizontal line and T_f at each P_n, which is equally spaced round the circumference, increases from P_n to P_{n+1} by θ. Applying the characteristics, let us define T_g at P_2 by revolving T_f around D by -θ. Then, it makes no influence to a chamfering condition. Besides, the tool can keep attitude near to the initial one by the rotation of -(n-1)θ at P_n.

As a result, the robot can be driven by the path with smaller changes in the attitude as shown in Fig. 14, and the tool attitude prevents the robot joints from reaching their limit of rotational angle. The tool path generated by the method is shown in Fig. 15.

5 Matching between the Coordinate Systems

The workpiece produced on the basis of CAD data can be placed arbitrarily on the table in front of the robot. A tool path generated in the workpiece coordinate system, as described in previous section, has to be converted to that in the robot coordinate system. However, the workpiece

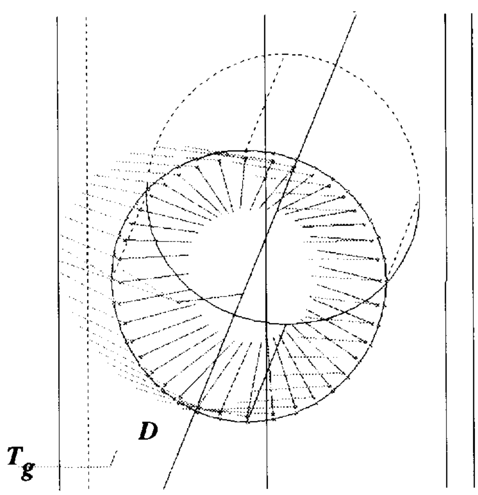

Fig. 15 Tool path based on the new method

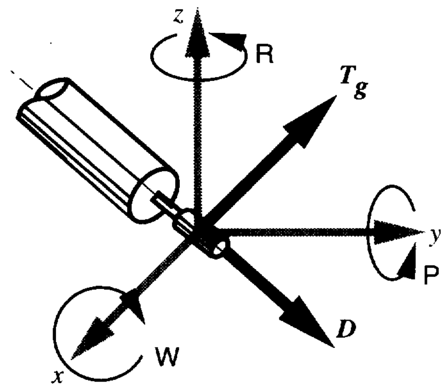

Fig. 16 Expression of tool attitude with angle

coordinate system has nothing to do with the robot coordinate one. The process, called "matching", relates these two coordinate systems each other. A touch sensor with a certain voltage, which is attached at the robot arm, makes contact with the workpiece, the voltage falls down to zero. This allows the robot to recognize the contact position. By use of the location information of the workpiece placed on the table, the tool position and the tool axis vector in the workpiece coordinate system is transformed to those in the robot coordinate system so that the system can generate the robot control commands necessary to control the robot movement.

6 Post-processor

The tool path is generated as a set of chamfering points and two vectors T_g and D, and is converted to the robot attitude expression since the robot used in the system has its own attitude expression. The attitude expression of robot, defined by W,P and R around x,y and z axes respectively, is shown in Fig. 16. Then, the extra tool path is added to the obtained tool path since the tool path generated in the previous section includes no path from the end of tool path to the beginning of the next one.

Finally, robot control commands are generated, taking account of a deburring speed and the mode such as chamfering or moving, and so on.

7 Experiment

A chamfering experiment was carried out to remove a burr along the edge of a hole on a cylindrical workpiece, which is difficult to chamfer with a simplified tool. The workpiece material is a plain carbon steel S45C, whose shape is a cylinder of 60 mm in diameter and a hole of 30mm in diameter, as shown in Fig. 17. The burr along the edge of the hole is about 1 mm in height. The chamfering conditions

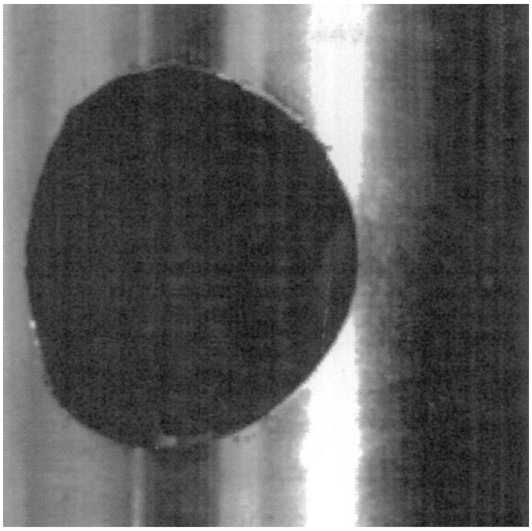

Fig. 17 Workpiece before chamfering

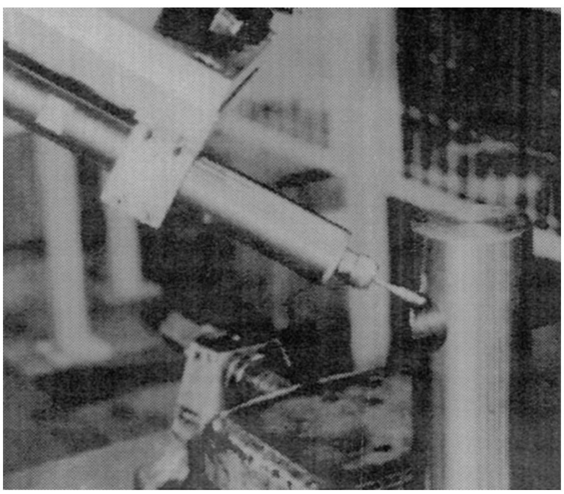

Fig. 18 Robot under chamfering

are follows; rotational speed of the tool : 35000 rpm, feed rate : 1.0mm/sec and depth of cut : 0.1 mm. The view of robot under chamfering is shown in Fig. 18. After several times repetition of the operation, the edge was chamfered by 1 mm in height as shown in Fig. 19, where the good chamfered edge can be seen.

8 Conclusion

The automatic chamfering system using an industrial robot is developed. The chamfering path is generated on the basis of CAD/CAM system. The system allows the chamfering tool to be set in a designated posture by 6-axis control. The system is experimentally found effective to remove a burr along the edge of a hole on a cylindrical workpiece considering robot arm attitude.

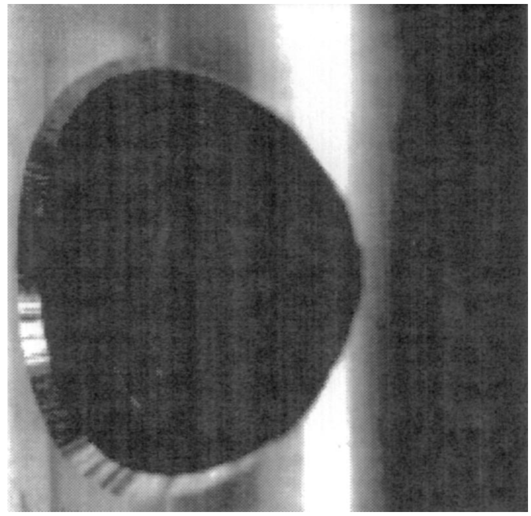

Fig. 19 Workpiece after chamfering

References

[1] G. Seliger, L. -H. Hsieh and G. Spur, Sensor-Aided Programming and Movement Adaptation for Robot-Guided Deburring of Castings, Annals of the CIRP, Vol.40/1 (1991) 487.

[2] H. Kazerooni, J. J. Bausch and B. M. Kramer, An Approach to Automated Deburring by Robot Manipulators, Trans. of the ASME, Vol.108, Dec. (1986) 354.

[3] T. M. Stepien, L. M. Sweet, M. C. Good and M. Tomizuka, Control of Tool/Workpiece Contact Force with Application to Robotic Deburring, IEEE Journal of Robotics and Automation, Vol.RA-3, No. 1 (1987) 7.

[4] M. A. Elbestawi, K. M. Yuen, A. K. Srivastava, and H. Dai, Adaptive Force Control for Robotic Disk Grinding, Annals of the CIRP, Vol.40/1 (1991) 391.

[5] M. G. Her and H. Kazerooni, Automated Robotic Deburring of Parts Using Compliance Control, Trans. of the ASME, Vol.113, Mar. (1991) 60.

[6] L. H. Chang and L. C. Fu, Nonlinear Adaptive Control of a Flexible Manipulatory for Automated Deburring, Proc. IEEE Int. Conf. on Robotics and Automation. (1997) 2844.

[7] G. M. Bone and M. A. Elbestawi, Sensing and Control for Automated Robotic Edge Deburring, Trans. of IEEE Industrial Electronics, Vol.41/2 (1994) 137.

[8] Y. Nonaka, S. Sakaue, Y. Yanagihara and K. Yokoshima, Development of an Impeller Grinding Robot System and a Gyro-moment Compensated Compliance Control, Proc. IEEE Int. Conf. on Robotics and Automation. (1995) 2084.